Peer-reviewed version available at Molecules 2019, 24, 2715; doi:10.3390/molecules24152715

Article

Enhanced nanoencapsulation of sepiapterin within PEG-PCL nanoparticles by complexation with triacetyl-beta cyclodextrin

Nataliya Kuplennik and Alejandro Sosnik[1,*]

[1] Laboratory of Pharmaceutical Nanomaterials Science, Department of Materials Science and Engineering, Technion-Israel Institute of Technology, Haifa, Israel

* Correspondence: Laboratory of Pharmaceutical Nanomaterials Science, De-Jur Bldg., Office 607, Department of Materials Science and Engineering, Technion-Israel Institute of Technology, 3200003 Haifa, Israel; Email: sosnik@technion.ac.il, alesosnik@gmail.com; Tel.: +972-(0)77-887-1971

Received: date; Accepted: date; Published: date

Abstract: In this work, we investigated for the first time the complexation of sepiapterin (SP), the natural precursor of the natural essential cofactor tetrahydrobiopterin, that displays mild water-solubility and short biological half-life, with the hydrophobic triacetyl-β-cyclodextrin (TAβCD) to improve its encapsulation within methoxy-poly(ethylene-glycol)-poly(epsilon-caprolactone) (mPEG-PCL) nanoparticles. First, TAβCD-SP complexes were produced by spray-drying of TAβCD/SP binary solutions by utilizing the Nano Spray Dryer B-90 HP. Then, dry powders were characterized by differential scanning calorimetry (DSC), Fourier-transform infrared spectroscopy (FTIR) and transmission and scanning electron microscopy (SEM and TEM, respectively) and compared to the complex components and physical mixtures (PMs). Next, SP was encapsulated within methoxy-poly(ethylene-glycol)-poly(epsilon-caprolactone) (mPEG-PCL) nanoparticles by nanoprecipitation of a SP/TAβCD complex/mPEG-PCL solution. In addition to complex nanoencapsulation, we assessed encapsulation of pure SP by nanoprecipitation with an intermediate step, which comprised the co-drying of SP, TAβCD and mPEG-PCL copolymer solution in organic solvent; this step aimed to promote the formation of molecular interactions between SP, TAβCD and the PCL blocks in the copolymer. SP-loaded mPEG-PCL nanoparticles were characterized by dynamic light scattering (DLS) and SEM. Nanoparticles with size of 74-75 nm and small polydispersity index (PDI <0.1) were obtained when SP-TAβCD equimolar spray-dried complex was used for nanoencapsulation, and SEM analysis indicated the absence of free SP crystals. Moreover, the encapsulation efficiency (*%EE*) and drug loading (*DL*) were 85% and 2.6%, respectively, as opposed to those achieved with pure SP encapsulation (14% and 0.6%, respectively). Overall, our results confirm that spray-drying of SP/TAβCD solutions at the appropriate molar ratio leads to the hydrophobization of the relatively hydrophilic SP molecule, enabling its encapsulation within mPEG-PCL nanoparticles.

Keywords: Sepiapterin; triacetyl-β-cyclodextrin (TAβCD); hydrophilic drug/cyclodextrin complexes; spray-drying; methoxy-poly(ethylene-glycol)-poly(epsilon-caprolactone) (mPEG-PCL) nanoparticles.

1. Introduction

Tetrahydrobiopterin (BH4, **Figure S1**), a naturally occurring molecule, is present in probably every cell or tissue of higher organisms and it is well-established as cofactor in various essential

Peer-reviewed version available at Molecules 2019, 24, 2715; doi:10.3390/molecules24152715

enzymatic pathways that include the degradation of phenylalanine and the biosynthesis of neurotransmitters such as serotonin, melatonin, dopamine, noradrenaline and adrenaline [1,2]. BH4 is also a key player in various biological processes associated with cardiovascular homeostasis and the immune response [1,3]. Defects in BH4 metabolism caused by congenital mutations in specific genes encoding for enzymes involved in its synthesis or regeneration and known with the general name of BH4 deficiency lead to the systemic deficiency of neurotransmitters in the CNS [4]. Moreover, decreased levels of BH4 have been also documented in neurological diseases such as Parkinson's disease, autism, depression and Alzheimer's disease. In some of them, administration of BH4 has been reported to improve the clinical symptoms [1,5]. However, BH4 undergoes fast aerobic degradation, which results in a decrease of the treatment efficacy [6]. BH4 deficiency is a disease with severe impact on neurological and cognitive development. In this framework, the development of advanced delivery systems that improve the biological half-life of BH4 and its bioavailability in the central nervous system (CNS) emerges as a strategy to enhance the efficacy of the current replacement therapy.

There exists a broad spectrum of synthetic biodegradable polymers used for production of nanoparticulate drug delivery systems that improve the physicochemical stability and sustain the release of hydrophobic cargos [7]. Among them, block copolymers made of hydrophilic components (e.g., poly(ethylene glycol), PEG) and hydrophobic polyester blocks such as poly(lactic acid) (PLA), poly(lactic-*co*-glycolic acid) (PLGA) and poly(epsilon-caprolactone (PCL) have gained major attention owing to the ability to fine-tune the hydrophilicity/lipophilicity and the thermal properties of the product and consequently to control the biodegradation and the release of the cargo in the biological environment [8–15]. However, BH4 is highly water-soluble (S_0 = 23 mg ml^{-1}) and extremely instable in water and air (**Figure S2**), precluding its encapsulation within polymeric nanoparticles.

Sepiapterin (SP, **Figure 1a**) is the natural precursor of BH4 and it is intracellularly converted into BH4 [16]. SP displays lower aqueous solubility (1.7 mg ml^{-1}) and higher chemical stability than BH4 and thus, it appears a good candidate to replace it in the design of advanced drug delivery systems. At the same time, encapsulation of relatively hydrophilic molecules within hydrophobic polymeric nanoparticles by utilizing conventional preparation methods remains a challenge and the development of new encapsulation procedures is called for [17,18].

The use of cyclodextrins to increase the aqueous solubility of hydrophobic drugs has been extensively investigated [19–22]. Recently, peracylated cyclodextrins (CDs) that are freely soluble in organic solvents and poorly water-soluble were proposed as excipients to decrease the water-solubility, prolong the biological half-life and sustain the release of hydrophilic drugs through the synthesis of water insoluble drug/CD complexes [23–27].

Aiming to encapsulate SP within polymeric nanoparticles as a platform for delivery and targeting, in this work, we synthesized for the first time a SP/triacetyl-β-cyclodextrin (TAβCD) (**Figure 1b**) complex by spray-drying SP/TAβCD binary solutions utilizing the Nano Spray Dryer B-90 HP. Then, dry powders were characterized by differential scanning calorimetry (DSC), Fourier-transform infrared spectroscopy (FTIR) and transmission and scanning electron microscopy (SEM and TEM, respectively) and compared to the pure complex components and SP/CD physical mixtures (PMs). Finally, the optimized complex was encapsulated within methoxy-poly(ethylene-glycol)-poly(epsilon-caprolactone) (mPEG-PCL) nanoparticles by a direct nanoprecipitation method. Overall results confirm the promise of this simple and scalable strategy for the nanoencapsulation of SP.

Peer-reviewed version available at Molecules 2019, 24, 2715; doi:10.3390/molecules24152715

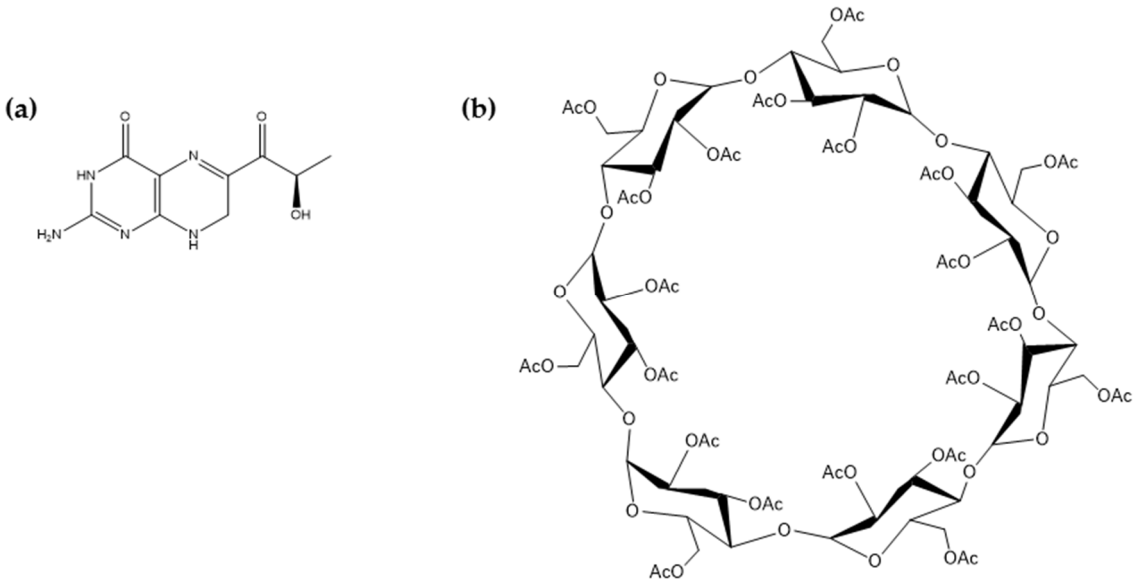

Figure 1. Chemical structure of (a) SP and (b) TAβCD.

2. Results and Discussion

2.1. BH4 and SP stability

BH4 (**Figure S1**) is known to undergo rapid degradation. Due to oxidation, BH4 solution becomes yellow. SP is known to be less sensitive to oxygen than BH4. The stability of BH4 and SP in deionized oxygen-free water (1% w/v) was investigated by UV/Vis spectrophotometry (**Figure S2**). The absorbance peak of BH4 at 266 nm decreased by 15% and red-shifted after 48 h, while a new absorbance peak at 329 nm appeared already after 1 h (**Figure S2a**). This also results in a change color to yellow. Conversely, SP remained stable even after 8 days, confirming that this precursor is much more stable than BH4 and a better candidate for encapsulation (**Figure S2b**). Moreover, the intrinsic solubility of BH4 in water is higher than of SP and thus, its encapsulation in hydrophobic polymers precluded. Thus, SP was chosen for further experiments, both due to higher stability and lower solubility.

For improvement of SP encapsulation within mPEG-PCL nanoparticles, we assessed two approaches: (i) drying of a solution of SP, TAβCD and mPEG-PCL copolymer in acetone prior to redissolution in acetone and nanoprecipitation and (ii) spray-drying of a solution of SP and TAβCD to obtain SP-TAβCD complex, and subsequent nanoprecipitation of the complexes and copolymers to obtain SP-encapsulated nanoparticles. Nanoprecipitaion in both approaches was performed according to the protocol described in the experimental section. Spray-dried SP/TAβCD complexes were further fully characterized to get an insight on interactions occurring between the two components.

2.2. Characterization of spray-dried SP/TAβCD complexes

In order to investigate possible SP/TAβCD interactions and exclude artifacts resulting from the sample preparation, pure TAβCD was subjected to the same procedure (dissolution and spray-drying) as binary SP/TAβCD solutions; this sample is named processed TAβCD. Pure SP was not spray-dried owing to its high cost as spray-drying requires relatively large amounts for sample collection. Instead, a reference sample (processed SP) was prepared by dissolution of SP in ethanol and drying under vacuum. Two SP:TAβCD molar ratios were used for complex preparation: equimolar (1:1) and with an excess of TAβCD (2:1) (**Table 1**). PMs of the pure components with the same molar ratios were prepared by grinding of dry TAβCD and SP using mortar and pestle.

Peer-reviewed version available at Molecules 2019, 24, 2715; doi:10.3390/molecules24152715

123 **Table 1.** Nomenclature of SP/TAβCD complexes and their PMs.

Preparation method	SP:TAβCD molar ratio	Nomenclature
Spray-drying (SD)	1:1	SP1/TAβCD1 SD
	1:2	SP1/TAβCD2 SD
Drying with copolymer (DWC)	1:1	SP1/TAβCD1 DWC
	1:2	SP1/TAβCD2 DWC
Physical mixture (PM(	1:1	SP1/TAβCD1 PM
	1:2	SP1/TAβCD2 PM

124

125 *2.2.1. Fourier-transform infrared spectroscopy*

126 FTIR spectra of SP, TAβCD, their PMs and the spray-dried samples are shown in **Figure 1**. Pure
127 and processed SP showed two bands at 3444 and 3377 cm^{-1} of N–H stretching vibration of primary
128 amine, a band at 3155 cm^{-1} due to the N–H stretching of secondary amine, and characteristic bands
129 at 1620 and 1590 cm^{-1} assigned to N-H bending of primary amine (**Figure 1**). TAβCD displayed very
130 strong bands at 1708, 1371, 1234 and 1045 cm^{-1} that correspond to C=O, -CH_3 and C-O-C vibrations
131 of the acetyl group (**Figure 1**) [28] . PMs spectra showed the overlapping of the bands of pure SP and
132 TAβCD and no significant shifts or depletion of the intensity of the characteristic bands with respect
133 to the pure components were observed. In contrast, FTIR spectra of the spray-dried SP/TAβCD
134 revealed a strong reduction or the complete disappearance of the characteristic SP bands in the 3800-
135 3000 cm^{-1} region, suggesting the interaction between SP and TAβCD and the formation of a complex.
136

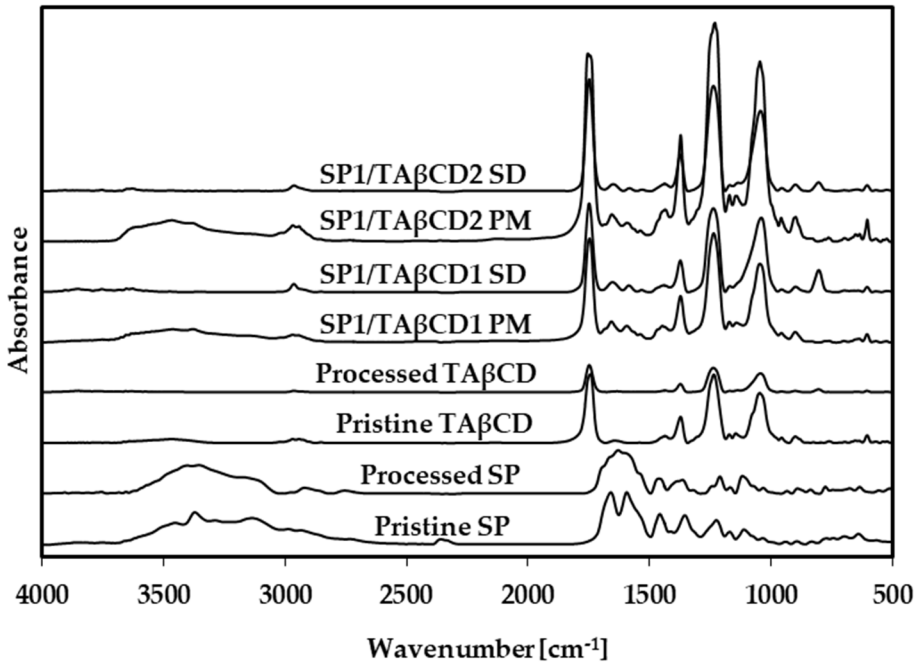

137 **Figure 1.** FTIR spectra of pristine and processed SP and TAβCD, their PMs and the SP/TAβCD
138 complexes obtained by spray-drying.

139 *2.2.2. Differential scanning calorimetry (DSC)*

140 DSC is widely used to study the interaction between a drug and a CD in the solid state
141 [20,29,30]. Thus, to further confirm the formation of a complex, we compared the thermal behavior
142 of pristine SP, SP/TAβCD PMs and spray-dried SP/TAβCD by DSC. Pristine TAβCD was

Peer-reviewed version available at Molecules 2019, 24, 2715; doi:10.3390/molecules24152715

characterized by a sharp melting endotherm at 223°C (**Figure 2**) associated with a melting enthalpy (ΔH_m) of 7.13 J g^{-1} (**Table 2**). Processed TAβCD thermal behavior differed from the pristine one; spray-dried TAβCD displayed an exothermic peak upon heating at 195°C due to the crystallization of amorphous TAβCD with a crystallization enthalpy (ΔH_c) of 8.4 J g^{-1} (**Figure 2**). The recrystallization of acetylated CDs that undergo amorphization during spray-drying was described elsewhere [31]. Then, recrystallized TAβCD melted at 220°C, though a smaller ΔH_m of 13 J g^{-1} than in pristine TAβCD (43 J g^{-1}) was observed (**Table 2**). This kind of behavior was also reported for TAβCD recrystallized from water/organic solvent solutions and indicates the partial amorphization of the CD [31]. Pure SP showed a more complex thermal behavior. A broad endotherm at 116°C (ΔH_m = 77.3 J g^{-1}) probably stemmed from the release of bound water (**Figure 2**, **Table 2**). Then, the beginning of melting was observed at 190°C followed by decomposition. Processed SP showed a similar profile, though the water-related peak of pristine SP was not apparent in the processed counterpart, suggesting the efficient elimination of water residues available in the original sample. However, the broad endotherm at 69°C probably corresponded to the evaporation of some solvent residues.

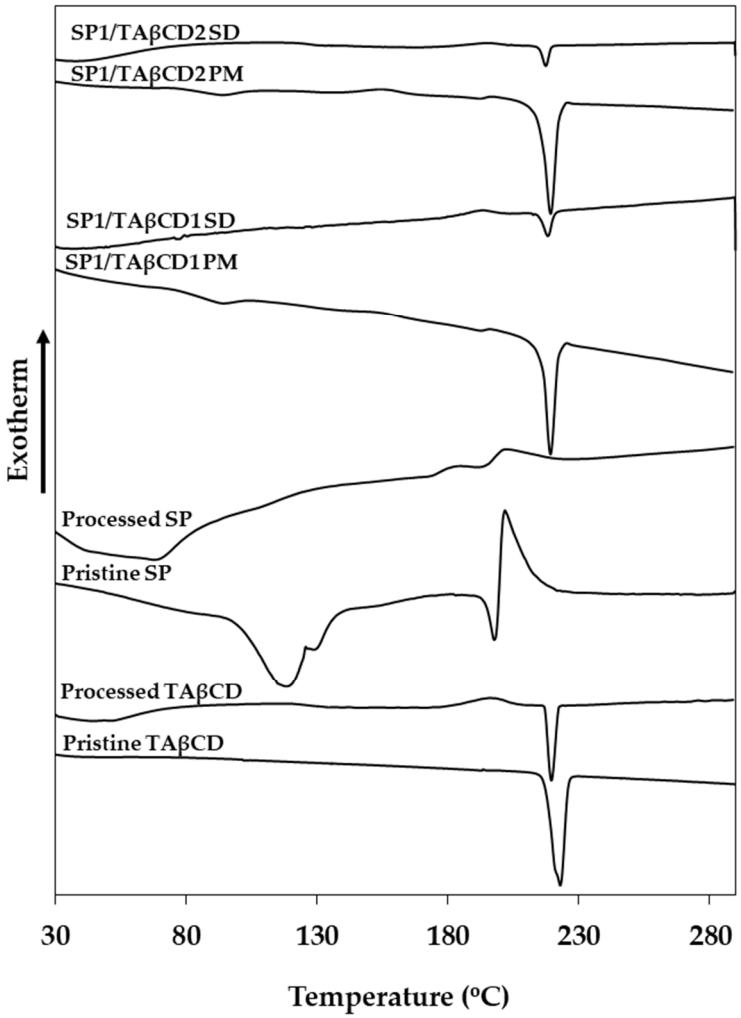

Figure 2. DSC thermograms of pristine and processed SP and TAβCD, their PMs and the complexes obtained by spray-drying.

The thermal analysis of PMs presented the endotherm associated with water release and the characteristic transitions of pure SP and TAβCD. TAβCD crystallization on heating at lower temperatures resulted from recrystallization of an amorphous form, obtained during the grinding in the preparation of PMs [26]. Appearance of weak endothermic peak at 190°C, followed by an

Peer-reviewed version available at Molecules 2019, 24, 2715; doi:10.3390/molecules24152715

exotherm, similar to that of pristine SP, was observed in both SP1/TAβCD1 and SP1/TAβCD2 PMs. However, due to relatively low weight fraction of SP in the samples, these peaks were less prominent compared to pristine SP. Such kind of thermal behavior of a drug in binary drug/CD PMs is typical of this kind of systems [32,33]. These observations suggest that there are no solid-state interactions between the two components in the PM. In contrast, DSC curves of the spray-dried SP/TAβCD complexes showed complete disappearance of the SP melting peak, and a strong reduction in the ΔH_m of TAβCD, indicating the total SP and the partial TAβCD amorphization, and the formation of a SP/TAβCD complex. In addition, considering that SP is a relatively hydrophilic molecule and that the cavity of TAβCD is hydrophobic, it is likely that SP/TAβCD form a non-inclusion complex.

Table 2. Thermal analysis of pristine and processed SP and TAβCD, spray-dried complexes and PMs, as determined by DSC. Enthalpy values were normalized to TAβCD and SP content.

Sample	TAβCD				SP	
	T_m [°C]	ΔH_m [J g^{-1}]	T_c [°C]	ΔH_c [J g^{-1}]	T_m [°C]	ΔH_m [J g^{-1}]
Pristine TAβCD	223	43	-	-	-	-
Processed TAβCD	220	13	195	8.4	-	-
Pristine SP	-	-	-	-	190 (with decomposition)	-
Processed SP	-	-	-	-	-	-
SP1/TAβCD1 SD	219	7.3	193	4.7	-	-
SP1/TAβCD1 PM	219	40	153	3.2	-	-
SP1/TAβCD2 SD	217	4.2	195	4.7	-	-
SP1/TAβCD2 PM	219	43	155	5.6	-	-

2.2.3. Morphological characterization of spray-dried complexes

Morphological characterization of the drug/CD complexes by electron microscopy is widely used [30,34]. Nevertheless, it should be mentioned that even if an apparent difference in crystallization state of the raw materials compared to the products exists, this characterization method should be used to confirm the formation of a complex only when combined with other chemical and thermal characterization methods [32]. The surface aspect of processed SP and TAβCD, their PMs and the spray-dried complexes were visualized by HR-SEM (dry powders) and TEM (powders re-suspended in water and casted). In HR-SEM, processed (spray-dried) TAβCD appeared as round-shaped amorphous particles (0.5-5 μm) (**Figure 3a**). In addition, processed SP showed irregular elongated needle-like crystals formed due to its crystallization during solvent evaporation. HR-SEM micrographs of SP/TAβCD PMs revealed the presence of the SP crystals dispersed in TAβCD (**Figure 3c,e**); no molecular interactions between the two substances in solid state were observed. Conversely, spray-dried mixtures appeared as round-shape particles, similar to spray-dried pristine TAβCD, with no visible SP crystals (**Figure 3d,f**). These results were consistent with DSC analysis and confirmed the amorphous nature of the spray-dried SP/TAβCD binary systems.

Peer-reviewed version available at Molecules 2019, 24, 2715; doi:10.3390/molecules24152715

192

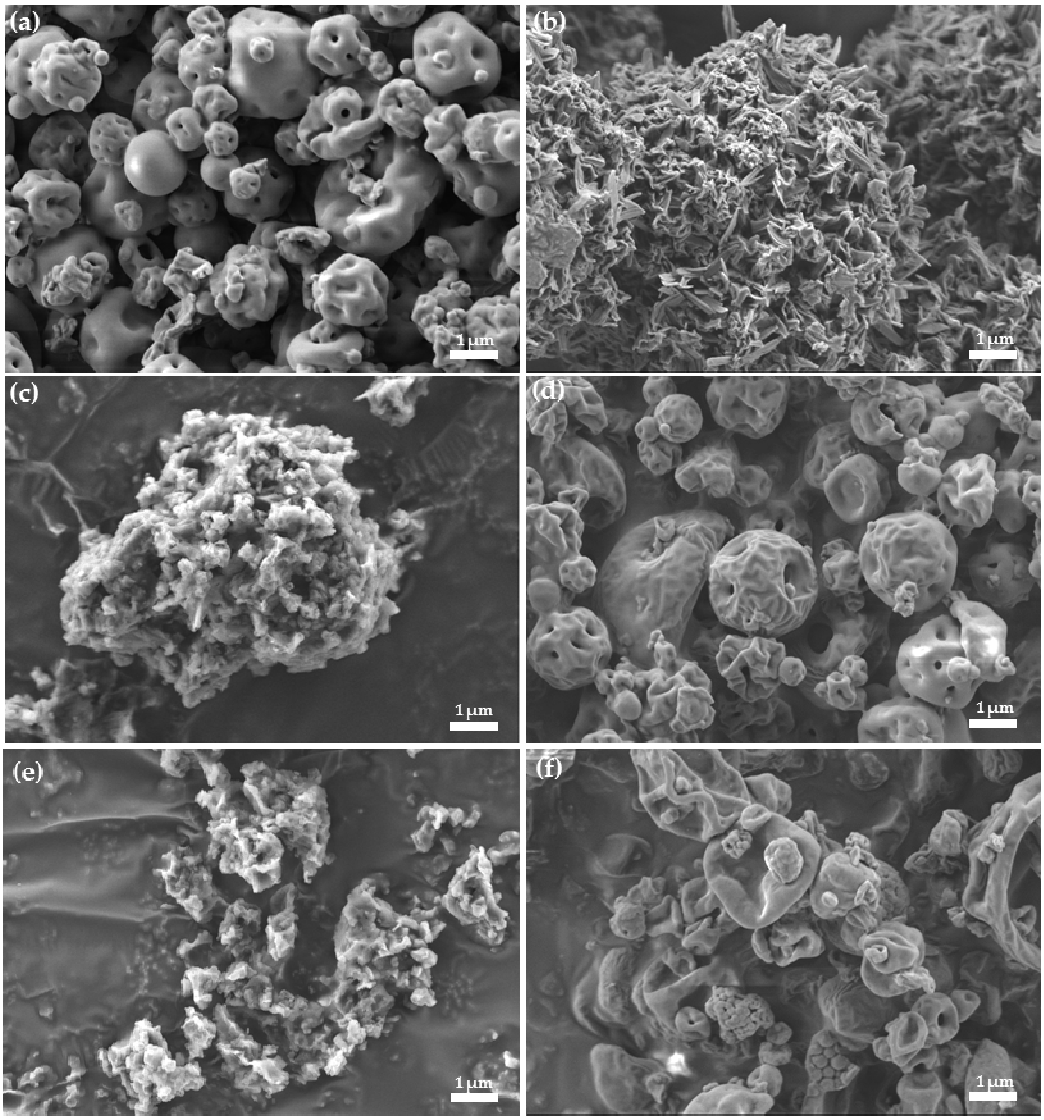

193 **Figure 3.** HR-SEM micrographs of (a) processed TAβCD, (b) processed SP, (c) SP1/TAβCD1 PM, (d)
194 spray-dried SP1/TAβCD1 complex, (e) SP1/TAβCD2 PM and (f) spray-dried SP1/TAβCD2 complex.

195 In addition, in TEM, processed TAβCD appeared as particles of irregular shape (**Figure 4a**),
196 while a processed SP sample produced by direct drop casting showed a needle-like crystalline
197 morphology (**Figure 4b**). These results were similar to those obtained in HR-SEM. Both SP/TAβCD
198 PMs showed the presence of square-shaped glassy chip structures that are typical for TAβCD (**Figure**
199 **4c,e**), while these structures were not observed in spray-tried complexes (**Figure 4d,f**) [31]. These
200 observations further supported that both components undergo amorphization during spray-drying.

Peer-reviewed version available at Molecules 2019, 24, 2715; doi:10.3390/molecules24152715

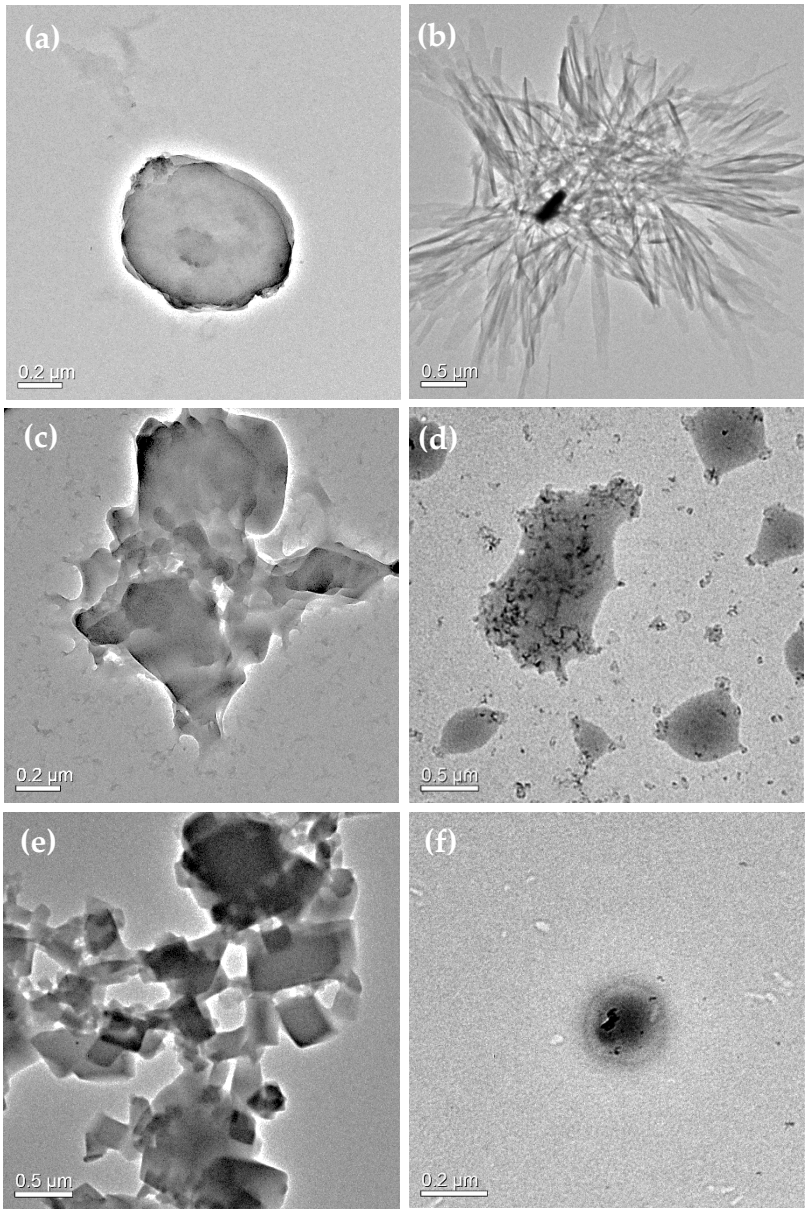

Figure 4. TEM micrographs of (A) processed TAβCD, (B) processed SP, (C) SP1/TAβCD1 PM, (D) spray-dried SP1/TAβCD1 complex, (E) SP1/TAβCD2 PM and (F) spray-dried SP1//TAβCD2 complex.

2.3. Production and characterization of SP-loaded nanoparticles

2.3.1. mPEG-PCL copolymer synthesis.

A mPEG-PCL copolymer with a relatively low hydrophilic-lipophilic balance was chosen as a model for nanoparticle production and synthesized by the ring opening polymerization (ROP) of epsilon-caprolactone (CL) initiated by the terminal hydroxyl group of a methoxy-terminated PEG with a molecular weight of 4000 g mol^{-1} in the presence of tin(II) 2-ethylhexanoate (SnOct) as catalyst at 145°C for 2.5 h and in the appropriate CL:mPEG molar ratio to obtain a PCL block of approximately 20,000 g mol^{-1} (**Figure S3**). The successful polymerization was confirmed by proton nuclear magnetic resonance spectroscopy (^{1}H-NMR) (**Figure S4**) and the number average molecular weight (M_n), the weight average molecular weight (M_w) and the dispersity (Đ, M_w/M_n) of the copolymer measured by gel permeation chromatography (GPC) (**Table S1**). **Figure S4** shows a representative ^{1}H-NMR spectrum of the obtained mPEG-PCL copolymer. The peak at δ = 3.60 ppm was assigned to the

Peer-reviewed version available at Molecules 2019, 24, 2715; doi:10.3390/molecules24152715

methylene (–CH_2) protons of the PEG chain. In addition, characteristic peaks of the methylene protons of the PCL block appeared at δ = 2.26, 1.61, 1.35, and 4.02 ppm. Since the number-average molecular weight of the PEG block used for the reaction is known from the supplier, the molecular weight of PCL block was calculated by taking the integration ratio of the characteristic peak of PEG (δ = 3.60 ppm) and PCL (δ = 2.26 ppm) (**Table S1**). In addition, the molecular weight of the copolymer was measured by GPC (**Table S1**). The experimental molecular weight was similar to the theoretical one.

2.3.2. Nanoencapsulation of SP.

Pristine SP was encapsulated within mPEG-PCL nanoparticles by a modified nanoprecipitation method performed under inert nitrogen conditions in a flask protected from light to prevent the possible oxidation of SP. Aiming to improve the SP loading within the nanoparticles, we assessed the encapsulation by utilizing two methods (**Figure 5**).

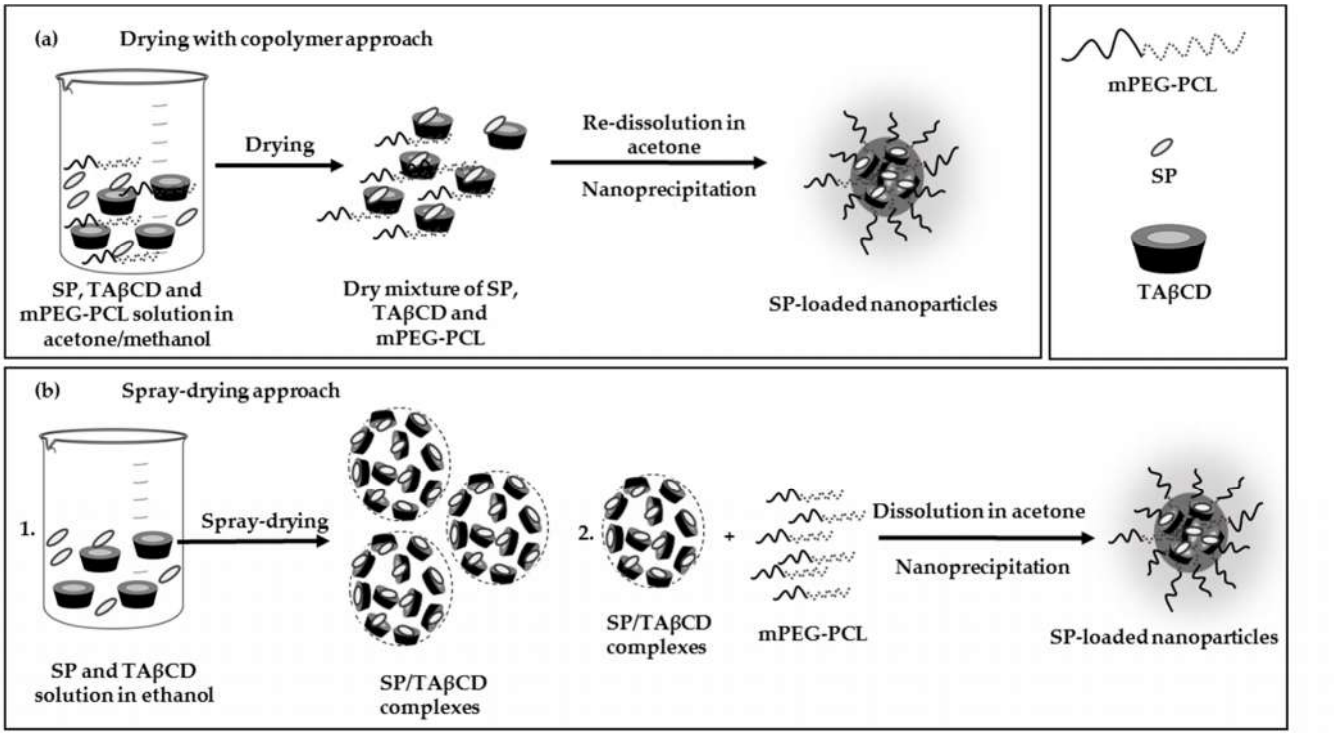

Figure 5. Method for the encapsulation of SP. (a) Drying of the SP, TAβCD with mPEG-PCL copolymer prior to nanoprecipitation and (b) co-dissolution of spray-dried SP/TAβCD complex with the copolymer and nanoprecipitation.

The first included dissolution of SP, TAβCD and the mPEG-PCL copolymer in organic solvent, drying, and re-dissolving in acetone with subsequent nanoprecipitation and nanoparticle formation (**Figure 5a**), while in the second, a spray-dried SP/TAβCD complex was co-dissolved with the copolymer and used for the nanoprecipitation (**Figure 5b**). It is worth stressing that equivalent amounts of each component were used, as depicted in **Table 3**.

Peer-reviewed version available at Molecules 2019, 24, 2715; doi:10.3390/molecules24152715

Table 3. Equivalent amounts of the different components used for the encapsulation of SP in mPEG-PCL nanoparticles.

Formulation	Equivalent amount used for encapsulation		
	mPEG-PCL [mg]	SP [mg]	TAβCD [mg]
Pure SP	50	2	-
		1	-
SP1/TAβCD1 DWC		2	17
		1	8.5
SP1/TAβCD2 DWC		2	34
		1	17
SP1/TAβCD1 SD		2	17
		1	8.5
SP1/TAβCD2 SD		2	34
		1	17

As for the first approach of preliminar dissolution of all three components and drying, we aimed to promote both the interactions between hydrophobic TAβCD and slightly more hydrophilic SP, as well as between hydrophobic PCL blocks of the copolymer and TAβCD and thus, increase the entrapment of SP molecules in the PCL/TAβCD matrix formed during the nanoprecipitation process with respect to TAβCD-free counterparts.

2.3.3. Size and size distribution of SP-loaded nanoparticles.

The size (hydrodynamic diameter, D_h) and size distribution (polydispersity index, PDI) of SP-free and SP-loaded nanoparticles produced by both methods, as well as suspensions of free TAβCD subtracted to nanoprecipitation at the same conditions, were measured by DLS (**Table 4**).

Table 4. Characterization of SP-loaded mPEG-PCL nanoparticles: size and size distribution (as measured by DLS), SP encapsulation yield and drug loading in the nanoparticles.

Formulation	**SP equivalent amount used for encapsulation [mg]**	**D_h [nm]* (± S.D.)**	**%Intensity**	**PDI (± S.D.)**	***%EE* [%] [a] (±SD)**	***DL* [%] [a] (±SD)**
TAβCD	-	312 (25)	100	0.231 (0.076)	-	-
SP-free nanoparticles	-	65 (3)	100	0.155 (0.030)	-	-
Pure SP	1	73 (3)	100	0.130 (0.024)	9 (1)	0.2 (0.1)
	2	83 (2)	100	0.099 (0.022)	14 (1)	0.6 (0.1)
SP1/TAβCD1 DWC	1	72 (7) 353 (71)	84 16	0.362 (0.069)	0 (0)	0 (0)
	2	100 (25) 4260 (226)	86 14	0.419 (0.051)	11 (1)	0.4 (0.1)
SP1/TAβCD2 DWC	1	105 (5)	100	0.270 (0.037)	7 (1)	0.1 (0)
	2	99 (14) 5066 (546)	77 23	0.749 (0.253)	9 (1)	0.3 (0)
SP1/TAβCD1 SD	1	74 (1)	100	0.094 (0.02)	62 (1)	1.1 (0.1)

Peer-reviewed version available at Molecules 2019, 24, 2715; doi:10.3390/molecules24152715

	2	75 (2)	100	0.091 (0.021)	85 (1)	2.6 (0.1)
SP1/TAβCD2 SD	2	69 (3) 312 (35) 4071 (852)	51 40 9	0.694 (0.067)	53 (1)	0.9 (0.1)
	1	72 (1) 5105 (496)	89 11	0.389 (0.093)	50 (1)	1.5 (0.1)

[a] Results are the average of 3 experiments (n = 3).

All the SP-loaded nanoparticles produced by the first approach, with the exception of the SP1/TAβCD2 formulation that used 1 mg of SP, showed two size populations: one major in the nanoscale (72-100 nm) and one minor in the microscale (4.2-5 μm) (**Table 4**). SP1/TAβCD2 DWC with 1 mg SP results in nanoparticles with monomodal size distribution and D_h of 105 nm. These results indicated the poor mixing between both hydrophobic components in the nanoparticles. In the case of spray-dried complexes, SP1/TAβCD1 resulted in nanoparticles with small size of 74-75 nm and PDI <0.1 (**Table 4).**

2.3.4. Encapsulation efficiency and drug loading.

Two parameters, the encapsulation efficiency (%*EE*) and the drug loading (*DL*) of SP in mPEG-PCL nanoparticles were quantified. For this, SP-loaded nanoparticle suspensions were washed thoroughly to remove residues of free TAβCD and SP, free SP quantified in the filtrate fraction and the %*EE* calculated according to **Equation 1**

$$\%EE = \frac{SP_{nanoparticle}}{SPt} \times 100\% \quad (1)$$

Where $SP_{nanoparticle}$ is the weight of SP in the nanoparticles and SP_t is the total weight of SP used in the encapsulation process.

In addition, the *DL* was calculated according to **Equation 2**

$$DL = \frac{SP_{nanoparticle}}{NPt} x\ 100\% \quad (2)$$

Where $SP_{nanoparticle}$ is the weight of SP in the nanoparticles and NP_t is the total weight of nanoparticles used for the quantification.

SP is hydrophilic and thus, its water-soluble nature makes it of difficult physical loading within hydrophobic mPEG-PCL nanoparticles, resulting in %*EE* and *DL* of 9-14% and 0.2-0.6% (**Table 4**). Similar or lower values were obtained with DWC systems. These results were consistent with DLS data, confirming that in this method, there is no effective entrapment of SP molecules within the PCL domains of the nanoparticle regardless of the presence of TAβCD molecules. When the CD was used to hydrophobize SP by spray-drying, both %*EE* and *DL* increased. In this context, the highest %*EE* and *DL* values (85% and 2.6%, respectively) were observed for SP-loaded nanoparticles produced with SP1/TAβCD1 SD and 2 mg of SP in the nanoprecipitation.

2.3.5. Morphological characterization of SP-loaded nanoparticles.

Representative SP-loaded nanoparticles were visualized using HR-SEM (**Figure 6**). For this, nanoparticles suspensions were drop-casted on silicon wafer. Upon water evaporation and drying of the sample, free SP crystallizes and forms needle-like crystals, similar to those observed during TEM analysis (**Figure 4b**). Free TAβCD can also undergo crystallization upon drying and form well-defined prismatic crystals or, conversely, to remain amorphous and form glassy chips [31]. As it can

Peer-reviewed version available at Molecules 2019, 24, 2715; doi:10.3390/molecules24152715

be seen, in SP-loaded nanoparticles prepared by the DWC method using 1 and 2 mg equivalent amounts of SP (**Figure 6a,b**, respectively), both SP and TAβCD crystals were observed, confirming the presence of free SP and TAβCD in the nanoparticle suspension. As for SP-loading nanoparticles prepared using spray-dried complexes, in case of TAβCD1-SP1 with 1 mg of SP, there were no SP or TAβCD crystals (**Figure 6c,d**). However, TAβCD2-SP1 produced with 1 mg of SP, several glassy TAβCD chips were seen. These findings indicated that a higher relative weight fraction of TAβCD used in the production of the complex with SP resulted in an excess of TAβCD which was not efficiently entrapped within the PCL matrix of the nanoparticle formed during the nanoprecipitation. In other words, the excess of TAβCD precluded the formation of stable mPEG-PCL nanoparticles. Overall these observations were in a good agreement with DLS data and confirmed that additional size populations observed in DLS analysis were associated with the presence of free or aggregated TAβCD.

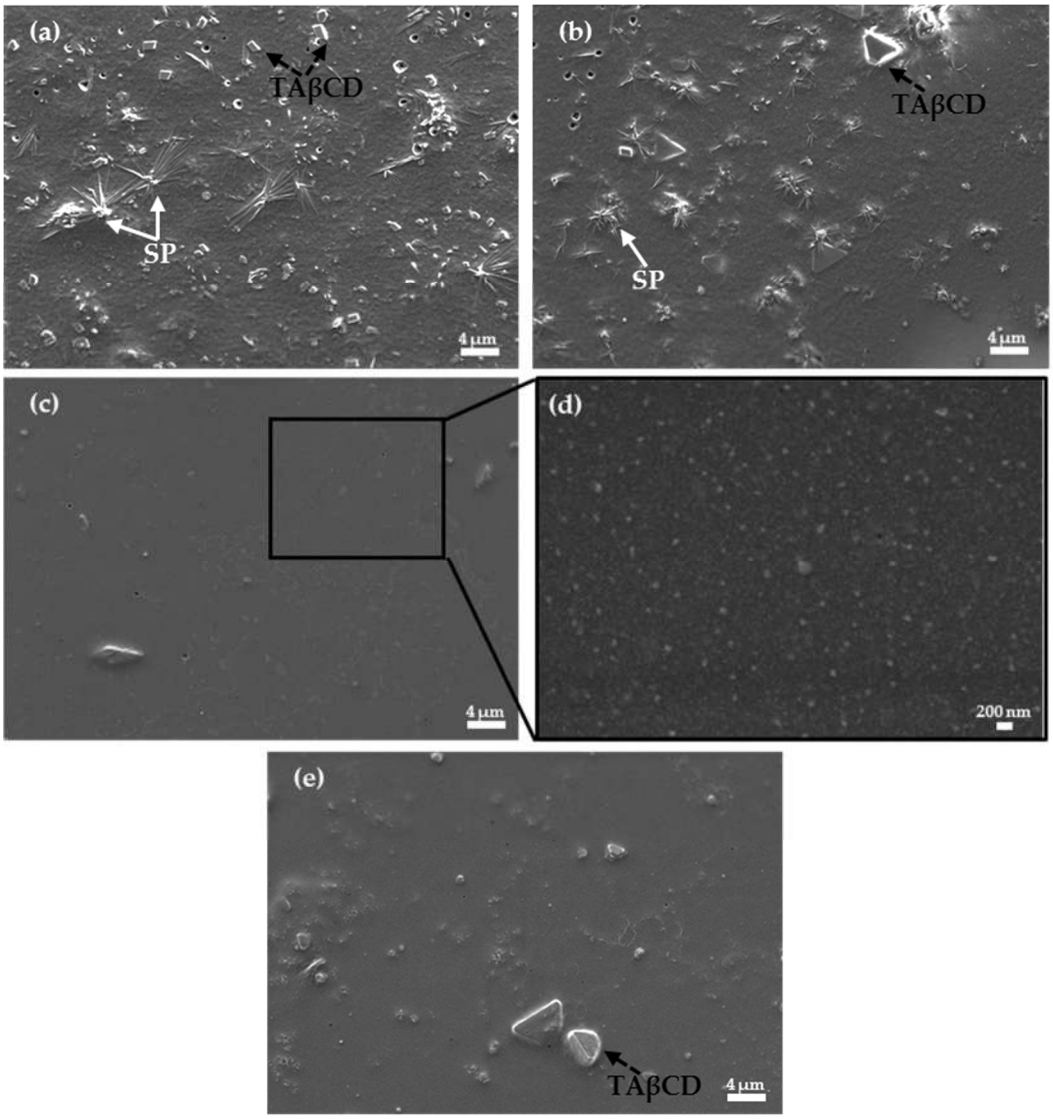

Figure 6. HR-SEM micrographs of SP-loaded mPEG-PCL nanoparticles utilizing (a) SP1/ TAβCD1 DWC (1 mg of SP), (b) SP1/TAβCD1 DWC (2 mg of SP), (c) encapsulation of spray-dried SP1/TAβCD1 complex (1 mg of SP) under x5K, (d) x50K magnification of (c) and (e) and encapsulation of spray-dried SP1/TAβCD2 complex (1 mg of SP).

Peer-reviewed version available at Molecules 2019, 24, 2715; doi:10.3390/molecules24152715

4. Materials and Methods

4.1. Preparation of spray-dried TAβCD-SP complexes.

TAβCD (85 or 170 mg for 1:1 and 1:2 SP/TAβCD complexes respectively; Sigma-Aldrich, St. Louis, MO, USA;) was dissolved in ethanol (19 and 38 mL for 1:1 and 1:2 complexes, respectively; Gadot, Netanya, Israel) with assistance of sonication in an ultrasonic bath (5 min, Elmasonic S 30, Elma Schmidbauer GmbH, Singen, Germany). SP (10 mg; Schricks Laboratories, Bauma, Switzerland) was dissolved in ethanol (12 mL) and mixed with the TAβCD ethanol solution. The resulting binary solution was stirred under heating at 55°C (10 min; Hei-Tec Magnetic Stirrer, Heidolph Instruments, Schwabach, Germany) in order to prevent TAβCD precipitation and subsequently spray-dried (Nano Spray Dryer B-90, Büchi Labortechnik AG, Flawil, Switzerland) using a closed loop configuration, under the following conditions: nitrogen flow 20 mL min^{-1}, an inlet temperature of 55°C, an outlet temperature of 60°C and 80% spraying. The obtained powder was kept in a sealed vial at 4°C and protected from light until use.

Pure TAβCD was spray-dried using the same method and named as processed TAβCD. A SP reference sample (processed SP) was also prepared by dissolution of SP (10 mg) in ethanol (12 mL) and drying under vacuum (Vacuum Oven Lab-Line Instruments Inc., Dubuque, IL, US); SP is thermo-sensitive and undergoes degradation.

4.2. Preparation of PMs

PMs of SP and TAβCD were prepared by mixing the pristine substances (1 mg of SP with 8.5 or 17 mg of TAβCD for 1:1 and 1:2 SP/TAβCD PM, respectively) using a geometric dilution method by continually grinding substances in a mortar and pestle.

4.3. Characterization of spray-dried SP/TAβCD complexes

Spray-dried SP/TAβCD complexes (SD SP/TAβCD) were fully characterized in order to confirm the formation of the complex and not of a PM.

4.3.1. Differential scanning colorimetry

DSC analysis was performed in a DSC 2 STAR^e system simultaneous thermal analyzer with STAR^e software V13 (Mettler-Toledo, Schwerzenbach, Switzerland) at a heating rate of 10°C min^{-1} in the 25–300°C temperature range under nitrogen flow of 20 mL min^{-1} and using In as standard.

4.3.2. Fourier-transform infrared spectroscopy

FTIR was recorded in an Equinox 55 spectrometer (Bruker Optics Inc., Ettlingen, Germany). Each sample (0.3% w/w) was thoroughly grinded with powdered KBr (Merck Chemical GmbH, Darmstadt, Germany) and compressed to a pellet under pressure of 10 MPa before the analysis. Spectra were obtained in the wavenumber range of 4000–500 cm^{-1} with a resolution of 4 cm^{-1} and 32 scans were performed for each spectrum.

4.3.3. Scanning electron microscopy

The surface morphology of the pure components and their binary combinations was visualized by HR-SEM (Zeiss Ultra-Plus FEG-SEM, Zeiss, Berkin, Germany), equipped with a high-resolution field emission gun. Samples were carbon sputtered prior to observation. The acceleration voltage was 2-4 kV. Images were obtained using secondary electron detector at 3-4 mm working distance.

4.3.4. Transmission electron microscopy

TEM was carried out in a Technai G2 T20 S-Twin (FEI, Eindhoven, Netherlands), operated at 200 kV. Samples were dissolved in water, followed by placing three 10 μL drops one after the other

Peer-reviewed version available at Molecules 2019, 24, 2715; doi:10.3390/molecules24152715

on a carbon grid (Formvar/Carbon 300 mesh; Electron Microscopy Sciences, Hatfield, PA, USA). Samples were finally dried in a fume hood overnight before analysis.

4.4. Preparation of SP-loaded mPEG-PCL nanoparticles

4.4.1. Synthesis of mPEG-PCL copolymer

A mPEG-PCL block copolymer was synthesized by a solvent-free melt ROP of CL (5 g; Sigma-Aldrich) initiated by the terminal hydroxyl group of mPEG of molecular weight 4000 g mol^{-1} (0.5 g; Tokyo Chemical Industry Co. Ltd. Tokyo, Japan). The polymerization was catalyzed by SnOct (142 µL, 1:200 molar ratio to CL, Sigma-Aldrich) and carried out at 145°C (2.5 h) under nitrogen atmosphere (**Figure S1**). After the reaction, the crude mixture was cooled down to room temperature, dissolved in dichloromethane (Gadot) and precipitated in an excess of diethyl ether (Bio-Lab Ltd., Jerusalem, Israel). The precipitated mPEG-PCL copolymer was filtered to remove remaining unreacted reagents, washed several times with diethyl ether, vacuum-dried at room temperature until constant weight and stored at -24ºC until use. The formation of the copolymer was determined by ^{1}H-NMR at 400 MHz utilizing a Bruker Avance III High Resolution spectrometer (Bruker BioSpin GmbH, Rheinstetten, Germany). The M_n, M_w and Đ (M_w/M_n) of the copolymer were determined by GPC (Alliance HPLC System, Waters Corp., Milford, MA, USA) with refractive index detector and 4 Styragel® HR (1-4) columns (7.8 X 300 mm, packed with 5 µm particles, Waters Corp.). The sample was prepared by dissolving mPEG-PCL copolymer (1% w/v) in tetrahydrofuran (THF, HPLC grade, Bio-Lab) and injecting 20 µL and the runs were conducted with a mobile phase flow of 1 mL min^{-1}, at 40°C. Poly(methyl methacrylate) standards (PSS polymer standards service, Mainz, Germany) with molecular weights between 2,260-171,000 g mol^{-1} were used for molecular weights calibration.

4.4.2. Drying of SP and TAβCD with mPEG-PCL copolymer

SP, TAβCD and mPEG-PCL, were dissolved in an acetone:methanol mixture (1:5 volume ratio) and magnetically stirred for 1 h at room temperature. Then, solvents were evaporated in a rotary evaporator (Rotavapor® R-100, Büchi Labortechnik AG) at room temperature and the dry solid mixture of SP, TAβCD and mPEG-PCL, was re-dissolved in anhydrous acetone. Nanoprecipitation was performed as described below.

4.4.3. Encpasulation of free SP and SD SP/TAβCD complexes in mPEG-PCL nanoparticles by nanoprecipitation

The encapsulation of pure SP and SD SP/TAβCD complexes in mPEG-PCL nanoparticles was performed using the nanoprecipitation method. In brief, the mPEG-PCL copolymer and SD SP/TAβCD complex (or pure SP) were dissolved in anhydrous acetone (10 mL) and the tertiary copolymer solution was added dropwise to degassed deionized distilled water (50 mL) in a sealed round-bottom flask under nitrogen flow to prevent the oxidation of SP due to exposure to air using a syringe pump (Laboratory Syringe Pump SYP-01, MRC Laboratory Equipment Manufacturer, Kfar Saba, Israel) at an injection rate of 0.333 mL min^{-1} and under magnetic stirring (480 rpm, Hei-Tec Magnetic Stirrer). Then, the acetone was evaporated using a rotary evaporator (Rotavapor® R-100), at room temperature. The nanoparticle suspension was kept in a sealed vial at 4°C and protected from light until use. The production of SP-free mPEG-PCL nanoparticles was carried out using the same method, though without the addition of SP and the CD.

Peer-reviewed version available at Molecules 2019, 24, 2715; doi:10.3390/molecules24152715

4.5. Characterization of SP-loaded nanoparticles

4.5.1. Size and size distribution

D_h and and PDI of the different nanoparticles were measured by means of DLS (Zetasizer Nanoseries ZS90, Malvern Instruments, Malvern, UK).

4.5.2. SP encapsulation efficiency and drug loading

For quantification of *%EE* and *DL* and, free SP was separated from the nanoparticles by ultrafiltration in Amicon® Ultra 15 mL Filters (MWCO 100 kDa, Merck Chemicals GmbH.). For this, each sample was centrifuged at 4500×g for 15 min at room temperature and SP was quantified in the filtrate fraction in a plate reader (Multiskan GO Microplate Spectrophotometer with SkanIt™ software, Thermo Fisher Scientific Oy, Vantaa, Finland) employing a calibration curve of SP in water built in a range between 10 and 100 μg ml^{-1} ($R^2 = 0.996$).

4.5.3. Morphological analysis of SP-loaded nanoparticles

Representative samples of SP-loaded nanoparticles were visualized by HR-SEM (Zeiss Ultra-Plus FEG-SEM). Samples were prepared by drop casting of 0.1% w/v nanoparticle suspension on a silicon wafer (CZ polished silicon wafers; SEH Europe Ltd., West Lothian, U.K.). Samples were carbon sputtered prior to analysis. The acceleration voltage was 2-4 kV. Images were obtained using secondary electron detector at 3-4 mm working distance.

Supplementary Materials: The following are available online at www.mdpi.com/xxx/s1
Figure S1. Chemical structure of BH4.
Figure S2. UV-Vis spectra of (a) pure BH4 and (b) pure SP solutions in water (1% w/v) at different times.
Figure S3: Ring opening polymerization of CL initiated by the hydroxyl groups of mPEG with molecular weight of 4000 g mol^{-1}.
Figure S34 ^{1}H-NMR spectrum of the mPEG-PCL copolymer in CDCl3.
Table S1: The number average molecular weight (M_n), the weight average molecular weight (M_w) and the dispersity (Đ, M_w/M_n), as determined by ^{1}H-NMR and GPC.

Funding: This work was supported by the Niedersächsisches Ministerium für Wissenschaft und Kultur & VolkswagenStiftung (Grant #88681). Partial support of the Russell Berrie Nanotechnology Institute (RBNI, Technion) is acknowledged.

Conflicts of Interest: The authors declare no conflict of interest

References

1. Thöny, B.; Auerbach, G.; Blau, N. Tetrahydrobiopterin biosynthesis, regeneration and functions. *Biochem. J.* **2000**, *347 Pt 1*, 1–16.
2. Thöny, B. Tetrahydrobiopterin and its functions. **2004**, 495–546.
3. Alp, N.J.; Channon, K.M. Regulation of Endothelial Nitric Oxide Synthase by Tetrahydrobiopterin in Vascular Disease. *Arterioscler. Thromb. Vasc. Biol.* **2004**, *24*, 413–420.
4. Hyland, K. Inherited Disorders Affecting Dopamine and Serotonin: Critical Neurotransmitters Derived from Aromatic Amino Acids. *J. Nutr.* **2007**, *137*, 1568S–1572S.
5. Blau, N.; Thöny, B.; Cotton, R.G.H.; Hyland, K. Disorders of tetrahydrobiopterin and related biogenic amines. In *The metabolic and molecular bases of inherited disease*; 2001; Vol. 2, pp. 1725–1776 ISBN 0079130356.
6. Davis, M.D.; Kaufm, S.; Milstein, S. The auto-oxidation of tetrahydrobiopterin. *Eur. J. Biochem.*

Peer-reviewed version available at Molecules 2019, 24, 2715; doi:10.3390/molecules24152715

1988, *173*, 345–351.

7. Sosnik, A.; Carcaboso, A.; Chiappetta, D. Polymeric Nanocarriers: New Endeavors for the Optimization of the Technological Aspects of Drugs. *Recent Patents Biomed. Eng.* **2010**, *1*, 43–59.
8. Moretton, M.A.; Glisoni, R.J.; Chiappetta, D.A.; Sosnik, A. Biointerfaces Molecular implications in the nanoencapsulation of the anti-tuberculosis drug rifampicin within flower-like polymeric micelles. *Colloids Surfaces B Biointerfaces* **2010**, *79*, 467–479.
9. Maitz, M.F. Applications of synthetic polymers in clinical medicine. *Biosurface and Biotribology* **2015**, *1*, 161–176.
10. Guo, J.; Gao, X.; Su, L.; Xia, H.; Gu, G.; Pang, Z.; Jiang, X.; Yao, L.; Chen, J.; Chen, H. Aptamer-functionalized PEG–PLGA nanoparticles for enhanced anti-glioma drug delivery. *Biomaterials* **2011**, *32*, 8010–8020.
11. Danafar, H.; Davaran, S.; Rostamizadeh, K.; Valizadeh, H.; Hamidi, M. Biodegradable m-PEG/PCL core-shell micelles: Preparation and characterization as a sustained release formulation for curcumin. *Adv. Pharm. Bull.* **2014**, *4*, 501–510.
12. Peng, W.; Jiang, X.; Zhu, Y.; Deng, W.; Yu, J.; Xu, X.; Zhang, W. Oral delivery of capsaicin using MPEG-PCL nanoparticles. *Acta Pharmacol. Sin.* **2014**, *36*, 139–148.
13. Riley, T.; Govender, T.; Stolnik, S.; Xiong, C.D.; Garnett, M.C.; Illum, L.; Davis, S.S. Colloidal stability and drug incorporation aspects of micellar-like PLA- PEG nanoparticles. *Colloids Surfaces B Biointerfaces* **1999**, *16*, 147–159.
14. Danafar, H. MPEG–PCL copolymeric nanoparticles in drug delivery systems. *Cogent Med.* **2016**, *3*, 1142411.
15. Grossen, P.; Witzigmann, D.; Sieber, S.; Huwyler, J. PEG-PCL-based nanomedicines: A biodegradable drug delivery system and its application. *J. Control. Release* **2017**, *260*, 46–60.
16. Pannirselvam, M.; Simon, V.; Verma, S.; Anderson, T.; Triggle, C.R. Chronic oral supplementation with sepiapterin prevents endothelial dysfunction and oxidative stress in small mesenteric arteries from diabetic (db/db) mice. *Br. J. Pharmacol.* **2003**, *140*, 701–706.
17. Massella, D.; Celasco, E.; Salaün, F.; Ferri, A.; Barresi, A.A. Overcoming the limits of flash nanoprecipitation: Effective loading of hydrophilic drug into polymeric nanoparticles with controlled structure. *Polymers (Basel).* **2018**, *10*.
18. Barichello, J.M.; Morishita, M.; Takayama, K.; Nagai, T. Encapsulation of Hydrophilic and Lipophilic Drugs in PLGA Nanoparticles by the Nanoprecipitation Method. *Drug Dev. Ind. Pharm.* **1999**, *25*, 471–476.
19. Londhe, A.S. and V. Inclusion Complexes of Hydroxy Propyl-beta-Cyclodextrin and Paliperidone: Preparation and Characterization. *Curr. Drug Discov. Technol.* 2014, *11*, 271–278.
20. Yang, H.; Parniak, M.A.; Isaacs, C.E.; Hillier, S.L.; Rohan, L.C. Characterization of cyclodextrin inclusion complexes of the anti-HIV non-nucleoside reverse transcriptase inhibitor UC781. *AAPS J.* **2008**, *10*, 606–613.
21. Loftsson, T.; Ólafsdóttir, B.J.; Friðriksdóttir, H.; Jónsdóttir, S. Cyclodextrin complexation of NSAIDSs: physicochemical characteristics. *Eur. J. Pharm. Sci.* **1993**, *1*, 95–101.
22. Loftsson, T.; Hreinsdóttir, D.; Másson, M. Evaluation of cyclodextrin solubilization of drugs. *Int. J. Pharm.* **2005**, *302*, 18–28.
23. Nakanishi, K.; Masukawa, T.; Nadai, T.; Yoshii, K.; Okada, S.; Miyajima, K. Sustained release

Peer-reviewed version available at Molecules 2019, 24, 2715; doi:10.3390/molecules24152715

of flufenamic acid from a drug-triacetyl-beta-cyclodextrin complex. *Biol. Pharm. Bull.* **1997**, *20*, 66–70.

24. Fernandes, C.M.; Veiga, F.J.B. Effect of the hydrophobic nature of triacetyl-beta-cyclodextrin on the complexation with nicardipine hydrochloride: physicochemical and dissolution properties of the kneaded and spray-dried complexes. *Chem. Pharm. Bull. (Tokyo).* **2002**, *50*, 1597–1602.
25. Fernandes, C.M.; Ramos, P.; Jose, F. Hydrophilic and hydrophobic cyclodextrins in a new sustained release oral formulation of nicardipine®: in vitro evaluation and bioavailability studies in rabbits. **2003**, *88*, 127–134.
26. Corti, G.; Capasso, G.; Maestrelli, F.; Cirri, M.; Mura, P. Physical – chemical characterization of binary systems of metformin hydrochloride with triacetyl- ® -cyclodextrin. **2007**, *45*, 480–486.
27. Nunes, A.V.M.; Almeida, A.P.C.; Marques, S.R.; Sousa, A.R.S. De; Casimiro, T.; Duarte, C.M.M. Processing triacetyl-β-cyclodextrin in the liquid phase using supercritical CO2. *J. Supercrit. Fluids* **2010**, *54*, 357–361.
28. Bratu, I.; Veiga, F.; Fernandes, C.; Hernanz, A.; Gavira, J.M. Infrared spectroscopic study of triacetyl-β-cyclodextrin and its inclusion complex with nicardipine. *Spectroscopy* **2004**, *18*, 459–467.
29. Ghorab, M.K.; Adeyeye, M.C. Enhancement of Ibuprofen Dissolution via Wet Granulation with β-Cyclodextrin. *Pharm. Dev. Technol.* **2001**, *6*, 305–314.
30. Carneiro, S.B.; Duarte, F.Í.C.; Heimfarth, L.; Quintans, J.D.S.S.; Quintans-Júnior, L.J.; Júnior, V.F.D.V.; De Lima, Á.A.N. Cyclodextrin-drug inclusion complexes: In vivo and in vitro approaches. *Int. J. Mol. Sci.* **2019**, *20*, 1–23.
31. Bettinetti, G.; Sorrenti, M.; Catenacci, L.; Ferrari, F.; Rossi, S. Polymorphism, pseudopolymorphism, and amorphism of peracetylated α-, β-, and γ-cyclodextrins. *J. Pharm. Biomed. Anal.* **2006**, *41*, 1205–1211.
32. Sami, F.; Philip, B.; Pathak, K. Effect of auxiliary substances on complexation efficiency and intrinsic dissolution rate of gemfibrozil-beta-CD complexes. *AAPS PharmSciTech* **2009**, *11*, 27–35.
33. Dollo, G.; Le Corre, P.; Chollet, M.; Chevanne, F.; Bertault, M.; Burgot, J.L.; Le Verge, R. Improvement in solubility and dissolution rate of 1,2-dithiole-3-thiones upon complexation with β-cyclodextrin and its hydroxypropyl and sulfobutyl ether-7 derivatives. *J. Pharm. Sci.* **1999**, *88*, 889–895.
34. Sapte, S.; Pore, Y. Inclusion complexes of cefuroxime axetil with β-cyclodextrin: Physicochemical characterization, molecular modeling and effect of l-arginine on complexation. *J. Pharm. Anal.* **2016**, *6*, 300–306.